UC Irvine
UC Irvine Previously Published Works

Title
Oxidation of CS2 and COS: sources for atmospheric SO2

Permalink
https://escholarship.org/uc/item/4mx3n0bk

Journal
Nature, 281(5728)

ISSN
0028-0836

Authors
Logan, Jennifer A
McElroy, Michael B
Wofsy, Steven C
et al.

Publication Date
1979-09-01

DOI
10.1038/281185a0

Copyright Information
This work is made available under the terms of a Creative Commons Attribution License, availalbe at https://creativecommons.org/licenses/by/4.0/

Peer reviewed

magnetic torque induced upon the white dwarf is $T \sim (4\pi/3)B_2 r_2^3 B_1 (r_1/R)^3 \sim 1 \times 10^{37}$, where the subscripts 1 and 2 refer to the primary and to the white dwarf, respectively. The resulting drag force is $F_d = T/R \sim 10^{24}$ dyn, which is the required value. If such coupling is dominant it would imply that SS433 is similar to the model of AM Her suggested by Stockman et al.[14]. Radio emission can easily arise in the lower regions of the white dwarf magnetosphere, with the X-ray emission being produced by infall onto the stellar surface[8].

We thank R. L. Brown, J. Liebert, R. O'Connell, S. O'Dell and R. Thompson for helpful discussion, and B. Margon for data. The National Radio Astronomy Observatory is operated by the Associated Universities Inc. under contract with the NSF and Kitt Peak National Observatory by the Association of Universities for Research in Astronomy Inc. under NSF contract.

1. Margon, B. *et al. Astrophys. J. Lett.* **230**, L41 (1979).
2. Margon, B. *et al. IAU Circ.* No. 3345 (1979).
3. Liebert, J. *et al. Astrophys. J.* (in the press).
4. Abell, G. O. & Margon, B. *Nature* **279**, 701–703 (1979).
5. Seaquist, E. R. *et al.* Preprint (1979).
6. Terlevich, R. J. & Pringle, J. E. *Nature* **278**, 719 (1979).
7. Fabian, A. C. & Rees, M. J. *Mon. Not. R. astr. Soc.* **187**, 13P (1979).
8. Angel, J. R. A. *Rev. Astr. Astrophys.* **16**, 487 (1978).
9. Liebert, J. *et al. Nature* **279**, 384–387 (1979).
10. Fabian, A. C. *et al. Mon. Not. R. astr. Soc.* **173**, 43 (1976).
11. McGraw, J. *et al. IAU Circ.* No. 3363 (1979).
12. Routh, E. J. *Dynamics of a System of Rigid Bodies*, 340–365 (Dover, New York, 1955).
13. Goldstein, H. *Classical Mechanics*, 182 (Addison, New York, 1950).
14. Stockman, H. S. *et al. Astrophys. J.* **217**, 815 (1977).

Oxidation of CS₂ and COS: sources for atmospheric SO₂

Jennifer A. Logan, Michael B. McElroy, Steven C. Wofsy & Michael J. Prather

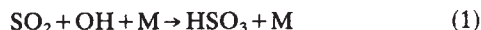Center for Earth and Planetary Physics, Harvard University, Cambridge, Massachusetts 02138

Oxidation of CS₂ and COS initiated by reaction with OH can provide a source of atmospheric SO₂ as large as 12 Mtonnes S yr⁻¹ and may represent the dominant source of SO₂ in remote regions of the marine troposphere.

EMISSION of sulphur associated with combustion of fossil fuel represents a major source of atmospheric pollution[1,2], contributing ~65 Mtonnes S yr⁻¹. Although the chemistry of sulphur in polluted atmospheres has been studied extensively, our knowledge of the natural cycle remains rudimentary. Measurements[3,4] at remote marine locations in the Southern Hemisphere indicate that the atmosphere contains a relatively constant background level of COS and SO₂. We shall argue here that SO₂ is derived at least in part from oxidation of COS, with additional sources due to CS₂ and dimethyl sulphide (DMS).
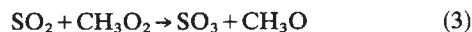
Sulphurous compounds in the atmosphere

It seems probable that the chemistry of sulphurous compounds in the troposphere should be dominated by reactions involving OH [5-7]. The hydroxyl radical is formed by reaction of $O(^1D)$ with H₂O, and is removed primarily by reaction with CO and CH₄. Results of model calculations for the concentration of OH are given in Fig. 1. We believe that concentrations shown here should be reliable to within about a factor of 2, and uncertainties of this magnitude should not qualitatively affect the arguments which follow.

Sulphur dioxide may be removed from the atmosphere by various heterogeneous processes[8], and by gas phase reactions[5,9] involving OH, HO₂ and CH₃O₂:

$$SO_2 + OH + M \rightarrow HSO_3 + M \tag{1}$$

$$SO_2 + HO_2 \rightarrow SO_3 + OH \tag{2}$$

and

$$SO_2 + CH_3O_2 \rightarrow SO_3 + CH_3O \tag{3}$$

The products in reactions (2) and (3) have not been measured directly, and these reactions may possibly involve formation of adducts. Reaction (1) has been studied by several groups[5,10], using a variety of techniques, and its rate constant is probably known to within about a factor of 2. It constitutes a major, perhaps dominant, path for removal of SO₂. Reaction (3) could be comparable to reaction (1). Considerable uncertainty attaches, however, not only to the mechanism of reaction (3), but also to the concentration of atmospheric CH₃O₂. Reaction (2) is of minor importance.

Studies of SO₂ in polluted air parcels[11,12] suggest an atmospheric lifetime of about a day. Calculations presented here for the marine atmosphere, using the kinetic data summarised in Table 1 but omitting heterogeneous reactions, indicate a lifetime of about 8 days. The difference may reflect in part the role of heterogeneous chemistry, in part omission of processes in polluted air which might be expected to result in higher concentrations of radicals (RO, RO₂). The calculations presented here were carried out using a one-dimensional photochemical model, as described by Logan et al.[13], with modifications to their chemical scheme as given in Table 1. Vertical profiles for O₃, CO, CH₄ and H₂O were specified using available observational data and calculations were performed for latitudes 45°N, 15°N, 15°S and 45°S.

Significant quantities of SO₂ may be formed during oxidation of COS and CS₂. It appears[6] that oxidation of COS should be initiated by reaction with OH,

$$OH + COS \rightarrow SH + CO_2 \tag{4}$$

Subsequent steps may involve production and removal of SO:

$$SH + O_3 \rightarrow HSO + O_2 \tag{5}$$

$$SH + O_2 \rightarrow SO + OH \tag{6}$$

$$SO + O_2 \rightarrow SO_2 + O \tag{7}$$

Rate constants for reactions (5)–(7) have not been determined experimentally. However, it seems reasonable that SH should be oxidised in the atmosphere to SO₂ by reactions (5)–(7) or by some other reaction mechanism. Measurements by Kurylo of the rate constant for reaction (4) and for the corresponding reaction with CS₂ are in conflict with results reported by Atkinson et al.[14]. Sources of the discrepancies are discussed in detail in ref. 6, and are attributed to complications due to photolysis of COS and to the occurrence of secondary reactions. Kurylo's experiments were performed in conditions designed to minimise these problems and his rate constants have been adopted accordingly. We estimate a global mean lifetime for COS of 200 days. Combining this lifetime with measured concentrations of COS[4,15], 0.5 ± 0.1 p.p.b. (parts per 10⁹, by volume) we infer a global destruction rate for COS equivalent to 4 ± 0.8 Mtonnes S yr⁻¹.

Oxidation of CS₂ can provide a significant source of COS[6,7], through

$$OH + CS_2 \rightarrow SH + COS \tag{8}$$

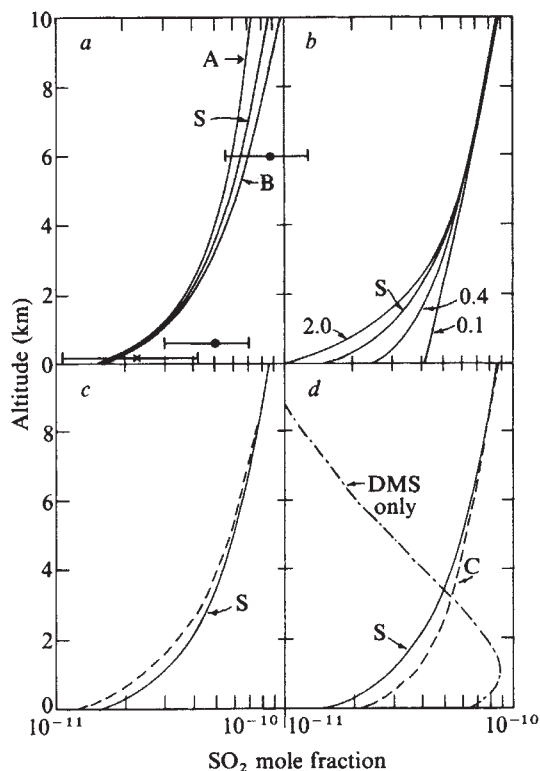Subsequent oxidation of SH, through reactions (5) and (6),

Fig. 1 Altitude profiles for OH and O_3 at 15° S latitude at equinox. *a*, Diurnally averaged concentrations for OH. The model calculations follow the time-dependent variation of short lived chemical species resulting from the diurnally varying radiation field which includes Rayleigh scattering. Calculations are shown for clear sky conditions (A) and a combination of clear sky (70%) and fully reflecting cloud layers at 3 km (17%) and 5 km (13%) (B). Vertical transport is simulated by 'eddy diffusion', with a diffusion coefficient equal to 10^5 cm^2 s^{-1}. The chemical model of Logan *et al.*[13] has been updated as described in Table 1. Fixed profiles for O_3[48] (see *b*), CO[49] (0.6 p.p.b.), CH$_4$[50] (1.5 p.p.b.) and H_2O (taken from the relative humidity values of Rasmusson[51]) were used. The mixing ratio of $NO + NO_2$ was taken to be 10^{-11} at 0 km, (ref. 52) and a deposition velocity of 1 cm s^{-1} was used for HNO$_3$. Note that the model implies a value of 1×10^6 molecules cm^{-3} for the globally averaged concentration of tropospheric OH.

should provide an additional source for SO_2. We estimate a lifetime for CS_2 due to reaction (8) of 60 days. Observational data for CS_2 are sparse, confined to the UK[15], and indicate a range of mixing ratios between 0.07 and 0.37 p.p.b. Sandalls and Penkett[15] point out that their data are consistent with the view that the ocean and atmosphere are in equilibrium with respect to CS_2. Using marine measurements of CS_2 by Lovelock[16], and solubility data by Seidell[17], they inferred an equilibrium concentration for the atmosphere equivalent to 0.22 ± 0.06 p.p.b. We adopt this value for the mixing ratio of CS_2 to represent global mean conditions. Used in conjunction with the chemical model of Table 1 and with the OH data of Fig. 1, it implies a global destruction rate for CS_2 equal to 12 ± 3 Mtonnes S yr^{-1}. The associated sources for COS and SO_2 are 6 ± 1.5 Mtonnes S yr^{-1} and 12 ± 3 Mtonnes S yr^{-1} respectively. Note that the source for COS due to oxidation of CS_2 could account for the bulk of atmospheric COS as discussed by Sze and Ko[7].

Source rates quoted here are directly proportional to values calculated for the concentration of OH. Studies of CH$_3$CCl$_3$[18,19] suggest that concentrations of OH given in Fig. 1 may be too high by about a factor of 2. If valid, this analysis would require corresponding reduction in source strengths inferred for CS_2 and COS. Relative abundances of CS_2, COS and SO_2 in remote locations are comparatively insensitive to details of the chemical model for OH, and provide a useful test of the hypothesis

proposed here, that is, that oxidation of CS_2 and COS might represent dominant background sources of SO_2. Our model predicts concentration ratios $CS_2:COS:SO_2$ at 6 km of $0.3:1.0:0.13$ which may be compared with observed ratios[4] of $0.44:1.0:0.17$. This is a fairly good agreement, when one remembers that the observational data for COS and SO_2 are uncertain to within about ±30%, that our value for the concentration of CS_2 was inferred from measurements of dissolved CS_2, and that the temperature dependencies of the rate constants for the key reactions (1), (4) and (8) are not well defined. In our model, one-half of the SO_2 source is derived from oxidation of CS_2, for which observational data are extremely limited. The mixing ratio for COS is fairly well defined and, given the uncertainties in the rate constants for reactions (1), (3) and (4), oxidation of COS alone might provide the major source for background SO_2.

Results and discussion

Calculated height profiles for SO_2 are shown in Fig. 2, which includes comparison with the observations by Maroulis *et al.*[4] and Nguyen Ba Cuong *et al.*[20]. We define a standard model, *S*, characterised by rate constants and parameters summarised in Table 1. Our choice of rate constant for reaction (1) is based on data reported by Castleman *et al.*[21] and Cox[22]. In their studies the rate for reaction (1) was measured relative to the rate for reaction of OH with CO. We applied suitable correction to account for the known pressure dependence[23] of $OH + CO$.

Our standard model assumes that the rate for reaction (1) is independent of temperature. Dependence of results on choice of rate expressions for reaction (1) is shown in Fig. 2*a*, which also includes models allowing modest negative activation energies
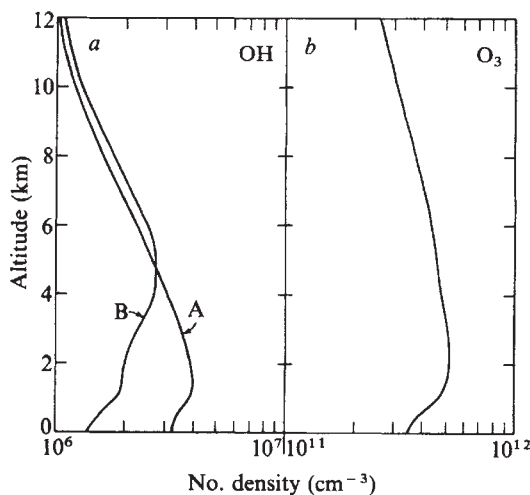

Fig. 2 Altitude profiles for SO_2 at 15° S latitude at equinox. The profiles were calculated with the model given in Fig. 1, curve B. The curves labelled S used the standard chemical model of Table 1, with a deposition velocity for SO_2 of 1 cm s^{-1} and a zero-flux boundary condition at the tropopause. The COS mixing ratio was specified at 0.5 p.p.b. Data are from Maroulis *et al.*[4] (●), aircraft flight over the Pacific Ocean, 0–67° S); and Nguyen Ba Cuong *et al.*[20] (x), Indian Ocean cruise, 5–25° S). *a*, The effect of temperature dependent rate constants: curve A, k_b (OH + SO_2) = 5.7×10^{-33} exp $(1,000/T)$; curve B, $k_4 = 3.4 \times 10^{-14}$ exp $(150/T)$, $k_8 = 1.1 \times 10^{-13}$ exp $(150/T)$. *b*, Uses the standard model *S*, but with values for the deposition velocity for SO_2 equal to 2.0, 0.4 and 0.1 cm s^{-1} as noted. *c*, The dashed curve includes loss of SO_2 to aerosols, with a sticking efficiency of 10^{-3}, as described in the text. *d*, The effect of a source of SO_2 from oxidation of DMS. Curve C includes an ocean source of DMS of 2.5 Mtonnes S yr^{-1}, in addition to SO_2 sources from CS_2 and COS oxidation, and may be considered as our best model. The curve labelled 'DMS only' omits all sources of SO_2 except that from DMS oxidation, and allows for a DMS source of 25 Mtonnes S yr^{-1}, the value suggested recently by Nguyen Ba Cuong *et al.*[37]. The calculated profiles of SO_2 exhibit small (<15%) variations with latitude between 45° N and 45° S.

for reactions (4) and (8). It seems probable that rates for reactions (4) and (8) should be faster at low temperature, given the reaction mechanism proposed by Kurylo[6,24]. The temperature dependence of k_1 is poorly determined. The rate expression given in Fig. 2a was based on preliminary work by Castleman and Tang[25] and Erler et al. (ref. 26 and results in ref. 10).

Figure 2b shows the dependence of calculated profiles for SO2 on the choice of deposition velocity, while Fig. 2c shows the possible influence of heterogeneous loss due to aerosols. The general behaviour of the profiles in Fig. 2a–c is similar. In all cases we find higher mixing ratios at high altitude, consistent with the observational data of Georgii et al.[27] and Maroulis et al.[4]. Uncertainties in loss processes tend to affect mainly concentrations computed for the lowest altitudes. Deposition velocities over land[8] are reported in the range 0.1–$2.0 \, \text{cm s}^{-1}$ while Hicks and Liss[28] suggest that a value of about $1 \, \text{cm s}^{-1}$ should be appropriate for moderate wind conditions at sea.

Results in Fig. 2c imply that loss of SO2 to aerosols should be relatively unimportant, at least in the marine atmosphere. We used an integrated surface area for aerosols equivalent to $1 \times 10^{-7} \, \text{cm}^2$ per cm^3, an estimate based on particle size distributions measured by Meszaros and Vissy[29], Blifford[30], and Jaenicke et al.[31]. We investigated sticking efficiencies for SO2 as high as 10^{-3}, although experimental data[32] suggest efficiencies much lower than this, in the range 10^{-3}–10^{-6}. Results in Fig. 2 do not allow for transient reductions in SO2 which might arise due to rainfall.

We assumed a rate constant for reaction (3) equal to $10^{-15} \, \text{cm}^3 \, \text{s}^{-1}$. With this choice, reaction (3) represents a relatively minor sink for SO2. Measurements by Kan et al.[33] indicate removal of CH3O2 by SO2, with an effective rate constant of 5–$10 \times 10^{-15} \, \text{cm}^3 \, \text{s}^{-1}$. If loss of CH3O2 observed in the laboratory is associated with the reaction channel (3), concentrations in Fig. 2 could be reduced by about 20%. This estimate assumes, however, an unproven model for oxidation of atmospheric CH4. It seems unlikely that k_3 should be as large as $10^{-14} \, \text{cm}^3 \, \text{s}^{-1}$ given the much smaller value, $\leqslant 10^{-17} \, \text{cm}^3 \, \text{s}^{-1}$ (refs 34, 58), reported for the analogous reaction (2).

Oxidation of DMS could provide an additional source of SO2 as suggested by Lovelock[35] and discussed further by Maroulis and Bandy[36] and Nguyen Ba Cuong et al.[37]. The associated source of SO2 would be confined to the lowest 2 km of the atmosphere as the reaction of DMS with OH is exceedingly rapid[38]. Thus DMS cannot account for the height profile observed for SO2, a point shown in Fig. 2d. Similar arguments apply to the suggestion that oxidation of H2S might produce a large source of SO2. Hydrogen sulphide also reacts very rapidly with OH[39], and concentrations as low as a few parts per trillion have been observed in tropical marine air[40]. Most estimates of the contribution of H2S to the atmospheric sulphur cycle have been derived by subtracting other terms in the budget for sulphur, and are consequently highly uncertain[1,2]. While biogenic sources of H2S and DMS may provide significant contributions to the atmospheric sulphur cycle in selected environments (for example, near swamps or salt marshes), these sources cannot account for the observations of SO2 discussed here.

Liss and Slater[41], using measurements by Lovelock et al.[35], estimate a net source of 3.7 Mtonnes S yr^{-1} associated with release of marine DMS, a source whose magnitude should be reduced by about a factor of 1.5 to account for more recent estimates of rates for gas exchange across the air–sea interface[42].

It seems probable that the concentrations of atmospheric CS2 and COS should reflect a combination of biogenic and industrial sources[43,44]. Preliminary measurements of the emission rates of sulphurous gases over salt marshes have shown that fluxes of COS might be comparable to, and in some cases greater than fluxes of H2S[45]. The relatively uniform distribution[4,13,46,47] observed for COS suggests a globally distributed source. This apparently argues against a significant industrial component, although there might be important production due to forest fires and combustion associated with land clearance for agriculture. The possibility of a dominant industrial component for CS2 cannot be excluded, given limitations in the present data base. It seems more likely, however, that diffuse sources should dominate for CS2 as well as for COS. These sources may include a component due to combustion although thermodynamic considerations suggest that reactions in reducing environments may be more important. It seems probable that these reactions should be microbially mediated: swamps, anaerobic muds and the digestive tracts of various animals offer plausible sites. The relatively uniform distribution observed for SO2 in the upper marine troposphere[4] requires a diffuse atmospheric source for

Table 1 Kinetic data

No.	Reaction	Rate expression*	Refs and notes
1	$OH + SO_2 + M \rightarrow HSO_3 + M$	$k_a = 6.8 \times 10^{-13}$ $k_b = 1.6 \times 10^{-31}$ $1/k = 1/k_a + 1/k_b M$ $k_1 = k \times (k_9 / 1.4 \times 10^{-13})$	Fit to the data of refs 21, 22
2	$HO_2 + SO_2 \rightarrow SO_3 + OH$	2.0×10^{-17}	34
3	$CH_3OO + SO_2 \rightarrow$ products	1.0×10^{-15}	See text
4	$OH + COS \rightarrow SH + CO_2$	5.66×10^{-14}	6
7	$OH + CS_2 \rightarrow SH + COS$	1.85×10^{-13}	6
8	$OH + (CH_3)_2 S \rightarrow$ products	$6.08 \times 10^{-12} \exp(134/T)$	38
9	$OH + CO \rightarrow CO_2 + H$	$2.10 \times 10^{-13} f(M) \exp(-115/T)$ $f(M) = (1 + 3.7 \times 10^{-20} \times M)$	53 23
10	$HO_2 + O_3 \rightarrow OH + 2O_2$	$1.40 \times 10^{-14} \exp(-580/T)$	Zahniser and Howard (personal communication)
11	$HO_2 + NO \rightarrow OH + NO_2$	$3.3 \times 10^{-12} \exp(254/T)$	54
12	$HO_2 + HO_2 \rightarrow H_2O_2 + O_2$	$3.9 \times 10^{-14} f(H_2O) \exp(1245/T)$ $f(H_2O) = 1 + 2.5 \times 10^{-18} \times [H_2O]$	55, 56
13	$H_2O_2 + h\nu \rightarrow OH + OH$		57
14	$CH_3OO + NO \rightarrow CH_3O + NO_2$	8.0×10^{-12}	Estimated
15	$CH_3OO + HO_2 \rightarrow CH_3OOH + O_2$	3.0×10^{-12}	Estimated
16	H_2O_2 heterogeneous loss (units, s^{-1})	1.16×10^{-5} 0–4 km $1.16 \times 10^{-5} \exp(1.6 - 0.4 \, z)$ 4–12 km	
17	$SO_2 + aerosol \rightarrow$ heterogeneous loss (probability)	0.0	†

* Units $\text{cm}^3 \, \text{s}^{-1}$ for bimolecular reactions; $\text{cm}^6 \, \text{s}^{-1}$ for termolecular reactions. The complete chemical scheme is described in Logan et al.[13].
† The integrated surface area for marine aerosols was taken to be $1.0 \times 10^{-7} \, \text{cm}^2$ per cm^3, and a scale height for the aerosol distribution function of 1 km was adopted (see refs 29–31).

this gas. Oxidation of COS and perhaps CS_2 as discussed here can provide a relatively straightforward explanation for the existence of a uniform background level of SO_2.

1. Friend, J. P. in *Chemistry of the Lower Atmosphere* (ed. Rasool, S. I.) (Plenum, New York, 1973).
2. Granat, L., Rodhe, H. & Hallberg, R. O. *Ecol. Bull.* **22**, 89–134 (1976).
3. Mészáros, E. *Atmos. Envir.* **12**, 699–705 (1978).
4. Maroulis, P. J., Torres, A. L., Goldberg, A. B. & Bandy, A. R. *Trans. Am. geophys. Un* **59**, 1081–1082 (1978); 1082 (1978).
5. Calvert, J. G., Su, F., Bottenheim, J. W. & Strausz, O. P. *Atmos. Envir.* **12**, 197–226 (1978).
6. Kurylo, M. J. *Chem. phys. Lett.* **58**, 238–242 (1978).
7. Sze, N. D. & Ko, M. K. W. *Nature* **280**, 308–310 (1979).
8. Garland, J. A. *Atmos. Envir.* **12**, 349–362 (1978).
9. Cox, R. A. *Phil. Trans. R. Soc. A* **290**, 543–550 (1979).
10. Moortgat, G. K. & Junge, C. E. *Pure appl. Geophys.* **115**, 759–774 (1977).
11. Prahm, L. P., Torp, U. & Stern, R. M. *Tellus* **28**, 355–372 (1976).
12. Nguyen, B. C., Bonsang, B., Lambert, G. & Pasquier, J. L. *Pure Appl. Geophys.* **113**, 489–500 (1975).
13. Logan, J. A., Prather, M. J., Wofsy, S. C. & McElroy, M. B. *Phil. Trans. R. Soc. A* **290**, 187–234, 1978.
14. Atkinson, R., Perry, R. A. & Pitts, J. N., Jr *Chem. phys. Lett.* **54**, 14–18 (1978).
15. Sandalls, F. J. & Penkett, S. A. *Atmos. Envir.* **11**, 197–199 (1977).
16. Lovelock, J. E. *Nature* **248**, 625–626 (1974).
17. Seidell, A. in *Solubilities of Inorganic and Metal Compounds, Vol. 1* (Van Nostrand, New York, 1940).
18. Singh, H. B. *Geophys. Res. Lett.* **4**, 453–456 (1977).
19. Lovelock, J. E. *Nature* **267**, 32 (1977).
20. Nguyen, B. C., Bonsang, B. & Lambert, G. *Tellus* **26**, 241–248 (1974); Cuong, B. C., Bonsang, B., Pasquier, J. L. & Lambert, G. *J. Res. Atmos.* **8**, 831–844 (1974).
21. Castleman, A. W., Davis, R. E., Munkelwitz, H. R. Tang, I. N. & Wood, W. P. *Int. J. Chem. Kin. Symp.* **1**, 629–640 (1975).
22. Cox, R. A. *Int. J. Chem. Kin. Symp.* **1**, 379–398 (1975).
23. Biermann, H. W., Zetzsch, C. & Stuhl, F. *Ber. Bunsenges. Phys. Chem.* **82**, 633–639 (1978).
24. Kurylo, M. J. & Laufer, A. H. *J. chem. Phys.* **70**, 2032–2033 (1979).
25. Castleman, A. W. & Tang, I. N. *J. Photochem.* **6**, 349–354 (1976).
26. Erler, K., Field, D. & Zellner, R. *4th Int. Conf. on Gas Kinetics* Edinburgh (1975).
27. Georgii, H. W. & Gravenhorst, G. *Pure appl. Geophys.* **115**, 503–511 (1977).
28. Hicks, B. B. & Liss, P. S. *Tellus* **28**, 349–554 (1976).
29. Mészáros, A. & Vissy, K. *J. atmos. Sci.* **5**, 101–110 (1974).
30. Blifford, I. H. *J. geophys. Res.* **75**, 3099–3103 (1970).
31. Jaenicke, R., Junge, C. & Kanter, H. J. *Met. Forsch. Ergebn.* **B7**, 1–54 (1971).
32. Judeikis, H. S., Stewart, T. B. & Wren, A. G. *Atmos. Envir.* **12**, 1633–1641 (1978).
33. Kan, C. S., McQuigg, R. D., Whitbeck, M. R. & Calvert, J. G. *Int. J. Chem. Kin.* (in the press).
34. Burrows, J. P., Cliff, D. I., Harris, G. W., Thrush, B. A. & Wilkinson, J. P. T. *W.M.O. Tech. Not. No.* 511, 25–28 (1978).
35. Lovelock, J. E., Maggs, R. J. & Rasmussen, R. A. *Nature* **237**, 452–453 (1972).
36. Maroulis, P. J. & Bandy, A. R. *Science* **196**, 647–648 (1977).
37. Nguyen, B. C., Gaudry, A., Bonsang, & Lambert, G. *Nature* **275**, 637–639 (1978).
38. Kurylo, M. J. *Chem. phys. Lett.* **58**, 233–237 (1978).
39. Perry, R. A. Atkinson, R. & Pitts, J. N. *J. chem. Phys.* **64**, 3237–3239 (1976).
40. Slatt, B. J., Natusch, D. F. S., Prospero, J. M. & Savoie, D. L. *Atmos. Envir.* **12**, 981–991 (1978).
41. Liss, P. S. & Slater, P. G. *Nature* **247**, 181–184 (1974).
42. Broecker, W. S. & Peng, T. -H. *Tellus* **26**, 21–35 (1974).
43. Crutzen, P. J. *Geophys. Res. Lett.* **3**, 73–76 (1976).
44. Peyton, T. O., Steele, R. V. & Mabey, W. R. *Stanford Res. Inst. Rep.* No. 68–01–2940 (1976).
45. Aneja, V. P., Overton, J. H., Cupitt, L. T., Durham, J. L. & Wilson, W. E. *Tellus* **31**, 174–178 (1979).
46. Hanst, P. L., Spiller, L. L., Watts, D. M., Spence, J. W. & Miller, M. F. *J. Air Pollut. Contr. Ass.* **25**, 1220–1226 (1975).
47. Maroulis, P. J., Torres, A. L. & Bandy, A. R. *Geophys. Res. Lett.* **4**, 510–512 (1977).
48. Chatfield, R. & Harrison, H. *J. geophys. Res.* **82**, 5969–5976 (1977).
49. Heidt, L. E., Krasnec, J. P. *Trans. Am. geophys. Un* **59**, 1077 (1978).
50. Ehhalt, D. H., Schmidt, U. *Pure appl. Geophys.* **116**, 452–464 (1978).
51. Rasmusson, E. M. in *The General Circulation of the Tropical Atmosphere and Interactions in the Extraterrestrial Latitudes* (ed. Newall, R. E., Ch. 5. MIT Press, 1972).
52. McFarland, M., Kley, D., Drummond, J. W., Schmeltekopf, A. L. & Winkler, R. H. *Geophys. Res. Lett.* **6**, 605–608 (1979).
53. Greiner, N. R. *J. chem. Phys.* **51**, 5049–5051 (1969).
54. Howard, C. J., & Zahniser, M. S. *J. chem. Phys.* (submitted).
55. Cox, R. A. *W.M.O. Tech. Note* No. 511, 17–27 (1978).
56. Hamilton, E. J. & Lii, R.-R. *Int. J. chem. Kin.* **9**, 875–885 (1977).
57. Molina, L. T., Schinke, S. D. & Molina, M. J. *Geophys. Res. Lett.* **4**, 580–582 (1977).
58. Graham, R. A., Winer, A. M., Atkinson, R. & Pitts, J. N. *J. Phys. Chem.* **83**, 1563–1567 (1979).

The effects of past variations of the Earth's rotation rate on climate

B. G. Hunt

Australian Numerical Meteorology Research Centre, PO Box 5089AA, Melbourne, Australia 3001

Palaeological evidence indicates that the rotation rate of the Earth during the late Precambrian was 2–2.5 times faster than now. Typically high rotation rate in a fluid system reduces the characteristic size of dynamic features, their associated transport processes and the overall intensity of the motions. The climatic consequences of the high rotation rate during the Precambrian are outlined. In particular, it is hypothesised that variations in the rotation rate imposed an important, and possibly dominant, effect on the genesis and termination of the Precambrian ice age. Other possible implications of the high rotation rate to oceanography, life forms and geology are briefly noted.

POTENTIAL mechanisms for producing climatic variations include solar perturbations owing to orbital variations of the Earth[1], volcanic activity[2], tectonic movements[3], fluctuations in solar output[4], glacier surgings[5] and oceanic feedback[6]. On a time scale of hundreds of millions of years a further factor, which has received relatively little attention[7], is the increase in the rotational period of the Earth. This increase is very small (~2.5 ms per century) and is still taking place. However, since the atmospheric and oceanic circulations are known to be critically influenced by the Earth's rotation rate it follows that climate should also be affected. Hence it is of value to consider what

impact past variations in the rotation rate might have had on the evolution of the Earth's palaeoclimate, and to see how well the deductions fit the known facts.

This assessment will be obtained by interpreting the results of a numerical model of the atmospheric circulation. This general circulation model of the atmosphere was hemispheric in extent, devoid of topography and thus oceanic influences, and was set up for fixed annual mean conditions[8]. Despite these apparently serious omissions the model is capable of a remarkable simulation of many features of the atmosphere[8,9], which encourages the belief that its application to problems concerned with variations in the rotation rate of the Earth has merit. This model has now also been run with the rotation rate increased and decreased by a factor of 5 as part of a spearate study[10], and it is this data base of three experiments which will be used here.

Prehistorical perspective

The rotational history of the Earth can be traced back to the late Precambrian era, about 1.5×10^9 yr ago. Based on growth patterns from shells and corals the Earth then had at least 800–900 solar days per yr, implying a rotation rate 2–2.5 times greater than the present value[11]. MacDonald [12] has calculated the past variation of the rotation rate and his results for one set of assumptions are shown in Fig. 1. This illustrates a possible increase in rotation rate with decreasing time up to about